

1 **Assessing the sources of particles at an urban background site using**
2 **both regulatory instruments and low-cost sensors – A comparative**
3 **study**

4
5 **Dimitrios Bousiotis¹, Ajit Singh¹, Molly Haugen³, David C.S. Beddows¹,**
6 **Sebastián Diez², Killian L. Murphy², Pete M. Edwards², Adam Boies³, Roy M.**
7 **Harrison¹ and Francis D. Pope¹**

8
9 **¹ Division of Environmental Health and Risk Management**
10 **School of Geography, Earth and Environmental Sciences**
11 **University of Birmingham, Edgbaston, Birmingham B15 2TT, United Kingdom**

12
13 **² Wolfson Atmospheric Chemistry Laboratories, Department of Chemistry, University of**
14 **York, Heslington, York YO10 5DD, United Kingdom**

15
16 **³ Department of Engineering, University of Cambridge, Trumpington Street, Cambridge, CB2**
17 **1PZ, United Kingdom**

18 **Abstract**

19 Measurement and source apportionment of atmospheric pollutants is crucial for the
20 assessment of air quality and the implementation of policies for its improvement. In most
21 cases, such measurements use expensive regulatory grade instruments, which makes it
22 difficult to achieve wide spatial coverage. Low-cost sensors may provide a more affordable
23 alternative, but their capability and reliability in separating distinct sources of particles have
24 not been tested extensively yet. The present study examines the ability of a low-cost Optical
25 Particle Counter (OPC) to identify the sources of particles and conditions that affect particle
26 concentrations at an urban background site in Birmingham, UK. To help evaluate the results,
27 the same analysis is performed on data from a regulatory-grade instrument (SMPS) and
28 compared to the outcomes from the OPC analysis. The analysis of the low-cost sensor data
29 manages to separate periods and atmospheric conditions according to the level of pollution
30 at the site. It also successfully identifies a number of sources for the observed particles, which
31 were also identified using the regulatory-grade instruments. The low-cost sensor, due to the
32 particle size range measured (0.35 to 40 μm), performed rather well in differentiating sources
33 of particles with sizes greater than 1 μm , though its ability to distinguish their diurnal
34 variation, as well as to separate sources of smaller particles, at the site was limited. The
35 current level of source identification demonstrated makes the technique useful for
36 background site studies, where larger particles with smaller temporal variations are of
37 significant importance. This study highlights the current capability of low-cost sensors in
38 source identification and differentiation using clustering approaches. Future directions
39 towards particulate matter source apportionment using low cost OPCs are highlighted.

40

41 1. Introduction

42

43 Particulate matter (PM) plays a dominant role in air quality and is known to cause adverse
44 health effects (Dockery et al., 1993; Pascal et al., 2013; Wu et al., 2016; Zeger et al., 2008). As
45 a result, regulatory limits are set for its concentrations, especially in urban areas (US EPA,
46 2012; WHO, 2006). For the implementation of such regulations, the identification of the
47 sources of PM is required. To accomplish this, measurements of the concentrations of PM,
48 typically alongside PM composition, in the area of study are conducted. Until recent years
49 these measurements were typically made using regulatory-grade instruments which, while
50 providing high quality data, are rather expensive thereby limiting the number that could be
51 deployed and consequently the spatial resolution of any measurement network. This
52 increases the spatial interpolation uncertainty (Kanaroglou et al., 2005) and can result in
53 inadequate connection between the levels of air pollution exposures and health effects
54 (Holstius et al., 2014), especially in complex urban environments (Harrison, 2017; Mueller et
55 al., 2016). Additionally, many low and middle income countries are unable to invest the large
56 economic assets currently required for source apportionment, even though in many of these
57 countries, the air quality is poor (Ghosh and Parida, 2015; Kan et al., 2009; Petkova et al.,
58 2013; Pope et al., 2018; Singh et al., 2020).

59 In the past decade, the development of new and cheaper sensors for air quality monitoring
60 has intensified. Many different sensors were introduced measuring either the number
61 concentration or surface area of PM, or the gas phase species (Jovašević-Stojanović et al.,
62 2015; Lewis et al., 2018; Popoola et al., 2018). Overall, the low-cost PM sensors currently offer
63 better comparison with regulatory grade equipment compared to their gas phase
64 counterparts (Lewis et al., 2018). However, many shortcomings have been identified in their
65 application, with the most common being the loss of accuracy in the measurements due to
66 environmental conditions such as relative humidity (RH) variations or high PM concentrations
67 (Castell et al., 2017; Crilley et al., 2018; 2020; Di Antonio et al., 2018; Hagan and Kroll, 2020,
68 Miskell et al., 2017; Zheng et al., 2018). Measurements in ambient conditions also lead to
69 discrepancies with research-grade instruments, which often measure in controlled
70 environments that are air conditioned (U.S. Environmental Protection Agency, 2016). The
71 reproducibility and variability of the outputs from sensors of the same type can also be

72 problematic (Austin et al., 2015; Sousan et al., 2016; Wang et al., 2015). Therefore, the need
73 for constant and careful calibration is repeatedly highlighted in many studies that evaluate
74 the potential of low cost sensors (Rai et al., 2017; Spinelle et al., 2015, 2017). When these
75 calibration steps are implemented, low-cost sensors have been shown to provide reliable
76 near-real time measurements, maintaining high correlations with research-grade instruments
77 (Kelly et al., 2017; Malings et al., 2020; Sayahi et al., 2019) with the added advantages of the
78 lower cost and portability.

79 Consequently, low-cost sensors have been successfully deployed in many studies for which
80 the use of more expensive instruments was not feasible. There is a number of applications in
81 low and middle income countries (e.g. Nagendra et al., 2019; Pope et al., 2018), in studies
82 which included mobile measurements within the urban environment (Ionascu et al., 2018;
83 Jerrett et al., 2017; Miskell et al., 2018), or studies of indoor air quality from multiple sites,
84 such as the SKOMOBO project conducted in New Zealand, in which the air quality in schools
85 was assessed (Weyers et al., 2018). The greatest advantage though is likely, as their name
86 implies, their lower cost which made possible the formation of a network of measuring
87 stations (Feinberg et al., 2019; Kotsev et al., 2016; Moltchanov et al., 2015), increasing the
88 spatial resolution and through new data analysis methods improve the mapping of air
89 pollution up to a sub-neighbourhood level (Schneider et al., 2017, Shindler, 2019). Therefore,
90 it is suggested that the development and use of low-cost sensors, either used individually or
91 in conjunction with research-grade instruments (Snyder et al., 2013), have the potential to
92 radically change the conventional approach of both pollution measuring and policy making
93 (Borrego et al., 2018; Kumar et al., 2015; Lagerspetz et al., 2019, Morawska et al., 2018),
94 providing a more effective general public information and enhanced environmental
95 awareness (Penza et al., 2014), even for countries with smaller budgets (Amegah, 2018).
96 As yet, studying the different sources of particles at a site with the use of data from low-cost
97 sensors has not been widely attempted yet. Pope et al., (2018) managed to identify major
98 pollution sources studying the ratios of PM of different sizes provided by low-cost sensors,
99 while Popoola et al., (2018) using a network of sensors identified the sources of pollution near
100 Heathrow airport in London, UK. Hagan et al., (2019) applying a statistical method (Non-
101 negative Matrix Factorisation) on low-cost sensor data, identified a combustion factor in a
102 three-factor solution in New Delhi, India. The present study investigates the ability of low-
103 cost sensors to provide measurements that can be used to identify the sources of pollution

104 at a background site in Birmingham, UK, using clustering of particle composition profiles. This
105 method was successfully used in a number of previous studies, though with the use of
106 measurements from research-grade instruments (Beddows et al., 2009, 2015; Von Bismarck-
107 Osten and Weber, 2014; Dall’Osto et al., 2011; 2012; Sabaliauskas et al., 2013). To support
108 the clustering method, chemical composition data from both research-grade and low-cost
109 sensor instruments were used, as well as meteorological data from a closely located
110 measurement station. Apart from attempting the source differentiation with low-cost sensor
111 data, a direct comparison with the results from a similar analysis using research-grade
112 instruments is also conducted to not only validate the results but find the strengths and
113 weaknesses of such an application.

114

115 **2. Methods**

116 **2.1 Location of the site and instruments**

117 The measurement site (fig. 1), characterised as an urban background, is the Birmingham Air
118 Quality Supersite (BAQS) located at the grounds of the University of Birmingham (52.45°N;
119 1.93°W), about 3 km southwest from the city centre (Alam et al., 2015). In the present study,
120 measurements from the following instruments for the period 24/01/2020 to 12/3/2020 (the
121 date range was chosen to avoid the effect of the lockdown due to COVID-19) were used (Table
122 1, a picture of the low-cost sensors used at BAQS is found in figure S1):

123 The Alphasense OPC-N3, which is an optical particle counter, measuring particle number
124 concentrations in the size range between 0.35 to 40 μm at rates up to about 10000 particles
125 per second. As the sample air stream enters the instrument with a sample flow rate of 210
126 mL m^{-1} (dynamically monitored and corrected by the sensor) it passes through a laser beam
127 (wavelength at 658 nm). The OPC-N3 measures the light scattered by individual particles
128 carried in a sample air stream through a laser beam. These measurements are used to
129 determine the particle size, related to the intensity of light scattered via a calibration based
130 on Mie scattering theory, and particle number concentration. Particle mass loadings (PM_1 ,
131 $\text{PM}_{2.5}$ and PM_{10}) are then calculated from the particle size spectra and concentration data,
132 assuming a particle density and refractive index (default density is 1.65 g/ml and refractive
133 index is 1.5+i0.). Particles of larger size are lost to impaction in the tubing prior to the OPC

134 and thus are not considered. The OPC is located within the air conditioned station, so
135 measurements represent PM dry mass.

136 The AethLabs MA200 (microAeth MA200) which provides black carbon (BC) information (0-1
137 mg BC/m³). The sample is deposited onto an internal filter, and an IR light (880 nm) is directed
138 through the sample on the filter and into a detector on the other side of the sample. The
139 amount of light absorbed from the sample is proportional to the BC concentration.

140 Two Naneos Partectors (Naneos Particle Solutions GmbH) which provide the lung deposited
141 surface area metric (LDSA, μm²/cm³) in the particle diameter range 10 nm to 10 μm. In
142 general, the provided data is dictated by the particle number concentration and diameter
143 (Nd^{1.1}) for both semi-volatile and solid particles. A catalytic stripper (Catalytic Instruments
144 CS015) was used to remove the semi-volatile particles entering one of the two Naneos
145 Partectors. The other Naneos Partector was not subject to the catalytic stripper and therefore
146 measured the surface of all particles. In the present study, apart from the values provided
147 directly from the sensors, the ratio between the measurements of the two Naneos Partectors
148 was also considered according to:

149

150
$$LDSA_{ratio} = \frac{LDSA \text{ after the catalytic stripper}}{LDSA \text{ before the catalytic stripper}}$$

151

152 This was done to resolve whether such a configuration can also provide information such as
153 the level of pollution or the age of the incoming air masses, as increased concentrations of
154 semi-volatile compounds are usually associated with anthropogenic sources, especially in the
155 urban environment (Harkov, 1989; Mahbub et al., 2011, Schnelle-Kreis et al., 2007, Xu and
156 Zhang, 2011). Thus, a high LDSA_{ratio} is expected to be associated with fresher pollution which
157 usually has a higher content of volatile compounds (i.e., pollution sources at a close distance
158 from the site), while lower ratios are probably associated with either cleaner conditions or
159 more regional and aged pollution with higher concentrations of semi-volatile compounds,
160 usually associated with sources at a greater distance from the measuring site. The specific
161 metric though should be considered with caution, as it can be biased by the absolute surface
162 areas measured.

163 The sensors monitoring nitrogen dioxide (NO₂) and ozone (O₃) concentrations are part of an
164 Alphasense Box Of Clustered Sensors (BOCS) (Smith et al., 2019), which is a low-power

165 instrument based on the clustering of multiple low-cost air pollution sensors allocated in two
166 independent circuits to redundantly measure concentrations and other airflow parameters.
167 The air is driven by a pump through the cell (air flow is about 4 L min^{-1}) that hosts the
168 electrochemical sensors (EC) and the nondispersive infrared sensors (NDIR). While the EC
169 sensors redundantly (6 sensors per gas) measure carbon monoxide, NO_2 , nitrogen monoxide,
170 oxidizing gases (O_x), the NDIR sensors measure carbon dioxide. EC sensors are based on
171 recording the current generated by redox reactions that occur at the electrode-electrolyte
172 interface in an electrochemical cell composed of three electrodes (working electrode (WE),
173 counter electrode (CE) and reference electrode (RE)). While the gas of interest reacts on the
174 WE surface, the CE completes the redox reaction and the RE ensures that the WE potential
175 remains in the proper range. In the present study, measurements of O_3 (deriving from a linear
176 regression of the values of the six O_x sensors with the measurements from the reference
177 instrument also located at BAQS) and NO_2 were only used from the specific sensor.

178 The Aethalometer model AE33 by Magee Scientific, collects aerosol particles continuously
179 by drawing the aerosol-laden air stream through a spot on the filter tape. It analyses the
180 aerosol by measuring the transmission of light through one portion of the filter tape
181 containing the sample, versus the transmission through an unloaded portion of the filter
182 tape acting as a reference area. This analysis is done at seven optical wavelengths spanning
183 the range from the near-infrared to the near-ultraviolet. The Aethalometer calculates the
184 instantaneous concentration of optically absorbing aerosols from the rate of change of the
185 attenuation of light transmitted through the particle-laden filter.

186 For the same period data from regulatory-grade instruments were also available. Thus,
187 particle size composition data from a model TSi3082 Scanning Mobility Particle Sizer (SMPS)
188 in the size range 12 – 552 nm, along with PM data for the sizes of 1, 2.5, 4 and 10 μm acquired
189 using a Fidas 200E were used. Additionally, chemical composition data for NO_2 , O_3 , as well as
190 SO_4^{2-} , NO_3^- and organic content (size range 40 nm to 1 μm) from an Aerodyne Aerosol
191 Chemical Speciation Monitor (ACSM) were also available. Meteorological data (wind speed
192 and direction, temperature, RH and rain level) from the Birmingham Air Quality Supersite
193 were also used in the characterisation of the clusters formed from both methods.

194 Planetary Boundary Layer (PBL) height data were downloaded from ECMWF's ERA5
195 (<https://cds.climate.copernicus.eu/cdsapp#!/dataset/reanalysis-era5-single-levels> - last
196 access 20/3/2021). Back trajectory data calculated using the HYSPLIT model (Draxler and
197 Hess, 1998), were extracted by the NOAA Air Resources Laboratory
198 (<https://ready.arl.noaa.gov/READYtransp.php> - last access 17/8/2020). Data was processed
199 using the Openair package for R (Carslaw and Ropkins, 2012).

200

201 **2.2 k-means clustering**

202 In this study, two size spectra are considered, one deriving from the OPC and one from the
203 regulatory-grade SMPS. It is noted that the size spectra from the two instruments only briefly
204 overlap in the size range 350 – 552 nm, with the SMPS mostly measuring smaller particles and
205 the OPC mostly measuring larger particles. For the period studied (24/1/2020 – 12/3/2020),
206 874 hours of available data (averaged from 10 second intervals - 76% coverage) from the OPC
207 and 732 hours from the SMPS (66% coverage) were exposed to k-means clustering. k-means
208 clustering is a method successfully used in many studies of particle source differentiation
209 (Beddows et al., 2015; Brines et al., 2015, Von Bismarck-Osten and Weber, 2014; Giorio et al.,
210 2015; Wegner et al., 2012) and was proven to have better performance compared to other
211 clustering techniques (Beddows et al., 2009; Salimi et al., 2014), as it was found to produce
212 clusters with the highest similarity between their elements and the highest separation against
213 the other clusters formed (Hennig, 2007). It is a method of vector quantisation which aims to
214 partition observations (x_1, x_2, \dots, x_n) into k sets, minimising within-clusters variances (squared
215 Euclidean distances) as:

$$216 \quad \arg \min \sum_{i=1}^k \sum_{x \in S_i} \|x - \mu_i\|^2 = \arg \min \sum_{i=1}^k |S_i| \operatorname{Var} S_i$$

217 where S_i are the sets (clusters) formed and μ_i are the centroid point of the cluster (Likas et al.,
218 2003). K-means clustering in this study was performed using the "stats" library for R. The
219 optimal number of clusters was chosen using two metrics, the Dunn Index and the Silhouette
220 width as proposed by Beddows et al., 2009. The Dunn Index provides a measure of the ratio
221 of the minimum cluster separation to the maximum cluster (providing a metric of the
222 compactness and separation of the clusters formed within the space – Pakhira et al., (2004)).
223 The larger the Dunn Index the better separated are the clusters formed. The Silhouette width

224 is a measure of the similarity of the spectra within each cluster (Rousseeuw, 1987). Both the
225 Dunn index and Silhouette width were calculated using the “fpc” library for R. In the present
226 study the best statistically fitted solution was chosen (the solution for which both metrics
227 maximised), though in source differentiation studies such a solution may not always provide
228 with the best separation of all the available sources. Using the aforementioned statistical
229 tests, a six-cluster solution was independently suggested for both the OPC and SMPS datasets.
230 Though the clustering process could be applied for the FIDAS data, which are comparable in
231 size range, it was not performed in this study.

232

233

234 **3. Results**

235 **3.1 General conditions, sources of particles and pollution at the site**

236 Being an urban background, the site studied presents relatively low concentrations of most
237 pollutants (the average atmospheric conditions for each cluster formed by both methods is
238 presented in table 2), without the effect of direct sources of pollution, such as traffic. Wind
239 rose and polar plots illustrating the conditions in the period studied are found in figure S2.
240 The main source of pollution lies on the north and northeast sectors, where the city centre is
241 located, as well as in the southern and eastern sectors where a populous residential area is
242 located. As a result, the main sources of NO_2 and BC as well as the smaller sized PM are
243 associated with easterly winds (this though is not reflected in particles observed in the SMPS
244 size range). For the PM_{10} apart from the aforementioned, increased concentrations are also
245 found with southwestern winds likely associated with marine sources. Typical for the UK, the
246 average wind profile for the period consists mainly of western and southwestern winds
247 (McIntosh and Thom, 1969), reducing the effect of the pollution sources in the east of the
248 site. Finally, the secondary pollutants NO_3^- and SO_4^{2-} which are in most cases associated aged
249 pollution and long-distance transport, have less consistent profiles, though they both seem
250 to be mainly associated with southern wind directions. Finally, for the period studied no New
251 Particle Formation events were observed. This is consistent with the general trend in the area
252 as found by Alam et al., (2003) for Birmingham (as well as in a more recent studies by Bousiotis
253 et al., (2019; 2021) at nearby sites in Oxford and London), in which NPF events in Southern

254 UK are more frequent during the summer months and barely occurring during winter and
255 early spring, mainly due to unfavourable meteorological conditions.

256

257 **3.2 Clustering of the OPC data**

258 Due to the larger particle sizes measured by the OPC-N3, the differences in the cluster profiles
259 are mainly associated with the particle number concentrations and to a lesser extent on the
260 different peaks, which are less distinct due to the smaller variation found as particle diameter
261 increases. The frequency of the clusters formed, and their diurnal occurrence is shown in
262 figure 2. The average particle size distribution spectra and wind roses for the clusters formed
263 are found in figures S3 and S4.

264 The six clusters formed from the OPC data are:

265 **OPC.1:** A rather polluted group with the highest NO₂ concentrations and average secondary
266 pollutants, PM and LDSA ratio. Its fresher polluted character is further confirmed using the
267 SMPS data which showed higher than average particle concentrations for particles with
268 diameter smaller than 50 nm. This group presents low average temperature, RH, PBL height
269 and slower than average southwestern winds, which is explained, to an extent, by the cluster
270 being slightly more frequent during night-time.

271 **OPC.2:** The second group refers mainly to a single midday event on 12/3/2020 (which explains
272 the highest PBL height found) with high-speed southwestern winds, which are associated with
273 lower pollution levels in the area (McGregor and Bamzelis, 1995), high temperature and very
274 low RH. On this day the concentrations of all the pollutants were rather low, though due to
275 the high wind speeds (an increase in the wind speed is observed at the start of the occurrence
276 of this cluster – at 10:00 AM - which affects the particle distribution profile as can be seen in
277 Figure S5) the PM₁₀ were close to average (when PM₁ and PM_{2.5} were rather low) indicating
278 the stronger presence of coarser particles, possible of marine origin as shown by the back
279 trajectories, a source with an increasing importance at larger size PM at this area (Harrison et
280 al., 2004; Taiwo et al., 2014). This group presents the highest LDSA ratio, which is in
281 agreement with the low concentrations of the secondary pollutants.

282 **OPC.3:** A group occurring mainly during some of the midday periods in January, with the
283 lowest temperature and wind speed averages, as well as the highest average RH, containing
284 both southwestern and southern winds. While the concentrations of the measured pollutants

285 are close to average, high sulphate and ozone concentrations were found, with the former
286 pointing to air masses with higher concentrations of aged pollutants assisted by the lowest
287 PBL found for this cluster. The LDSA ratio though, was found to be very high despite the higher
288 concentrations of sulphate and nitrate. The near average NO_2 concentrations may point to
289 the effect of a nearby pollution source that may resulted to the increased LDSA ratio found.

290 **OPC.4:** A group with low concentrations of NO_2 , BC and PM, but close to average secondary
291 pollutants' concentrations. It is associated with close to average temperature, RH, PBL height
292 and wind speed of mainly southwestern directions. It is slightly more frequent during daytime
293 and has lower than average concentrations of particles in the SMPS range.

294 **OPC.5:** This group includes the most polluted conditions in the area throughout the day. It is
295 associated with western and southwestern winds of average speed, high temperature and
296 lower than average RH. Most pollutant concentrations, including PM, are rather high while
297 O_3 is low. Similarly, it presents the highest concentrations of particles in all SMPS size ranges
298 which is probably due to the reduced atmospheric mixing in the lowest average PBL height
299 among the OPC clusters. This cluster also includes the more polluted conditions found with
300 north-eastern winds.

301 **OPC.6:** A group associated with rather clean conditions, presenting the lowest concentrations
302 of NO_2 , BC, NO_3^- and organic content. It is associated with higher than average temperature,
303 PBL height and wind speed and lower than average RH, and has low concentrations of PM_{1}
304 and $\text{PM}_{2.5}$, while PM_{10} concentration is close to average. Its association with cleaner
305 conditions (lower concentrations of the pollutants with available data) probably explains the
306 highest O_3 concentrations. The fast-moving southwestern air masses, which this group is
307 associated with, are probably of marine origin that have not passed through any significant
308 pollution sources, which can be further suggested by both the low LDSA values and the
309 highest LDSA ratio.

310

311 **3.3 Clustering of the SMPS data**

312 In the past, a number of studies on the sources of particles were conducted for both the
313 greater area of Birmingham and specifically the site in the University (Harrison et al., 1997;
314 Taiwo, 2016; Yin et al., 2010). As, these studies mainly focused on the chemical composition
315 of coarser particles, to the authors' knowledge this is the first study that uses ultrafine particle

316 size distribution data to study the sources of particles in Birmingham, UK. The frequency and
317 hourly occurrence of the six clusters formed from the SMPS data is found in figure 3. The
318 average particle size distributions and wind roses for the clusters formed are found in figures
319 S6 and S7.

320 **SMPS.1:** This group contains averagely polluted hours and is associated with fresher
321 pollutants (such as NO_2 or NO) and PM, while secondary pollutants such as NH_4^+ , NO_3^- and
322 SO_4^{2-} are relatively low. Due to being associated with fresher emissions this group presents
323 higher than average concentrations of particles below 50 nm and a low LDSA ratio. It is
324 associated with average speed southwestern winds (it also includes the small portion of
325 north-eastern winds) and temperature, higher than average RH and occurs more frequently
326 during late night and early morning hours, which explains the low PBL height among the SMPS
327 clusters.

328 **SMPS.2:** Similar to the first group, average pollutants' concentrations are found in this group
329 with low concentrations of secondary pollutants. It is associated with slow western and
330 southwestern winds, lower than average temperatures, RH and PBL height and is more
331 frequent during early morning hours. It has the highest concentrations of particles with
332 diameter smaller than 20 nm, but the particle concentrations become relatively smaller as
333 their size increase.

334 **SMPS.3:** This is a small group containing very clean night hours mainly in February, with higher
335 than average temperature, lower than average RH, strong western and southwestern winds
336 and a remarkably great PBL height for the time of the day. It has low concentrations of
337 pollutants and PM apart from O_3 (despite the time of day), though PM_{10} concentration is
338 enhanced, probably associating this group with stronger marine origins. The particle
339 concentrations of all size ranges below 500 nm are the lowest among the groups formed and
340 along with the high LDSA ratio are in agreement with the very clean conditions associated
341 with this cluster. This cluster, contrary to all other, presents two peaks: one peaking just
342 below 30 nm and another one just over 100 nm, which indicates that it is probably associated
343 with at least two different sources.

344 **SMPS.4:** This group presents near average concentrations of all the pollutants studied. PM_1
345 average concentration is rather low while PM_{10} is higher than the average. It is associated
346 with average speed southwestern winds, higher average temperature and PBL height and low

347 RH. It is more frequent during midday and evening hours and it appears to represent the most
348 common conditions in the area, hence having the highest frequency of all clusters.

349 **SMPS.5:** This is a unique group associated with southern winds, the side at which the central
350 part of the University resides. This is the most polluted group, probably affected by emissions
351 from the University and the residential area found in that direction assisted by the very low
352 PBL height, with very high concentrations of all the pollutants (apart from O_3), PM and
353 ultrafine particles with available data. The LDSA ratio is very high and this is probably due to
354 the great surface area of the involatile component found. It is associated with very slow wind
355 speeds, low temperature, very high RH and occurred evenly throughout the day, mainly on
356 the first weeks of the campaign when pollution levels were rather high, probably due to
357 increased heating emissions.

358 **SMPS.6:** This group presents low concentrations of all pollutants (apart from O_3), PM and
359 ultrafine particles with available data and is associated with western winds with higher than
360 average speed, near average temperatures and PBL height and low RH. It occurred more
361 frequently during evening hours and almost equally frequently throughout the whole study
362 period apart from the first 2 weeks when pollution levels were rather high.

363

364 **3.4 Direct comparison between the methods**

365

366 Due to the difference in the size ranges measured by the SMPS and OPC instruments, it is
367 evident that a direct comparison between the two methods would provide mixed results as
368 some clusters found using the SMPS data are not detectable with the OPC, and vice versa.
369 The particle size range that is common between the two instruments lies at about 350 – 550
370 nm. Therefore, many particle sources associated with particles in the size range below the
371 minimum detectable size of the OPC are not expected to be found using its data and vice
372 versa. At a background site though, many of the sources of smaller sized particles play a less
373 important role as they are usually associated with fresher emissions, which are not common
374 to such sites.

375 The clustering process attempts to separate the particle size distributions into groups with as
376 similar spectral profiles as possible, while being as different to the other groups as possible.
377 As expected, the SMPS is more capable in separating different cluster profiles at the size range

378 smaller than 500 nm, a size range in which the cluster profiles (using the SMPS data) formed
379 by the groups from the OPC are almost uniform (fig. 4). This shows the limitation of the OPC
380 data to distinguish ultrafine particle variations and thus it does not provide insight for the
381 sources of particles within this size range. On the other hand, the OPC performs much better
382 in identifying different sources when considering larger particles in the range between 1 – 10
383 μm , for which it manages to clearly distinguish variations between the groups formed (fig. 5).
384 The clusters formed using the OPC data appear to be better associated with different sources
385 of PM_1 (fig. 6), compared to those deriving from the SMPS data (fig. S8), as distinct “hot spots”
386 of PM_1 are more clearly defined on the polar plots from the OPC compared to the less clear
387 and mainly associated with calm (or almost calm) conditions from the SMPS (providing no
388 separation among possible sources of PM_1).

389 Table 3 contains the cluster relationships between the two methods, while Table S1 contains
390 the conditions observed when pairs of clusters from both methods are considered. The OPC.2
391 and OPC.3 clusters appear infrequently, and it would be nonsensical to directly associate
392 them with SMPS groups, as they appear under very specific conditions, that either are not
393 detected or are not identified as separate cases by the SMPS. As a result, they will be
394 separately studied later in this study.

395 The OPC.1 was mainly associated with SMPS.4 and SMPS.6 and to a lesser extend with
396 SMPS.1. OPC.1 has a somehow higher frequency during night times and it shares many of
397 these hours with groups SMPS.4 and SMPS.6, while with SMPS.1 it mainly shares early
398 morning hours. It includes the more polluted portion of the rather clean SMPS.6 and a portion
399 with lower PM_{10} (though not much difference from average pollutants’ concentrations) from
400 the more polluted SMPS.4. It is interesting that the variation between the subgroups (in
401 relation to SMPS clusters) of the OPC.1 is very small for the NO_2 concentrations, a pollutant
402 for which its variations are not expected to be directly “visible” at the size range of the OPC
403 as it is mainly associated to fresher emissions. No great variation was found for the wind
404 direction in the subgroups of OPC.1, though it includes the lower temperature and higher RH
405 conditions of the SMPS clusters it is associated with. The OPC.1 includes the relatively clean
406 part of the more polluted SMPS.1 and the more polluted portion of the cleaner SMPS.6. While
407 this does not provide a clear connection between the OPC and SMPS results, it shows that
408 there is consistency in the results provided by the former in identifying particle sources of
409 specific qualities.

410 Similarly, OPC.4 was mainly associated with SMPS.4 and SMPS.6. As the OPC.4 occurs under
411 cleaner conditions, it includes the less polluted hours of both the SMPS clusters it is mainly
412 associated with, though the concentrations of the secondary pollutants such as NO_3^- and SO_4^{2-}
413 are closer to the average. The OPC.4 is associated with the cleaner portion of the
414 aforementioned SMPS clusters with higher average temperature and RH though with variable
415 wind speeds.

416 OPC.5 represents a polluted group of hours associated mainly with SMPS.4, SMPS.5 and
417 SMPS.6. Being a group of hours associated with higher concentrations of pollutants, it
418 includes the more polluted portions of SMPS.4 and SMPS.6 with average meteorological
419 conditions, though lower wind speeds. It also coincides with the largest portion of SMPS.5,
420 mainly in the sixth week when the temperature was the lowest, including the portion with
421 the higher concentrations organic content and NO_3^- . SMPS.5 is the group that is associated
422 with southern wind directions, a side from which a source of secondary pollutants (NO_3^- , SO_4^{2-} ,
423 NH_4^+), organic content and particles of diameter greater than 100 nm occurs. The OPC.5 is
424 associated with the part of SMPS.5 which is more burdened from secondary pollutants, hence
425 very large concentrations are observed for them.

426 Finally, OPC.6 is mainly associated with SMPS.2, SMPS.4 and SMPS.6. Being a cleaner group
427 of hours, it includes the portion of these SMPS clusters with lower pollutant concentrations
428 but higher PM_{10} concentrations (though with lower PM_1 concentrations). These rather clean
429 conditions, along with the western and southwestern high-speed winds in average and the
430 large PM_{10} concentrations, further enhance the possible marine character of this cluster. Due
431 to the size range of these particles such variation is not clearly identified by the SMPS,
432 resulting to them not being clearly separated when its data is considered.

433 The weekly contribution of each cluster group from the analysis of either dataset is found in
434 Figure 7 and the conditions on each week studied in Table S2. It is evident that the variation
435 from the SMPS is greater than that of the OPC, as the latter is less affected by the diurnal
436 variations. It is apparent that it is easier to comprehend the clusters' variation in association
437 with the levels of pollution in the site (the more polluted weeks have a greater portion of
438 SMPS.1 and SMPS.5), while for those with lower concentrations of pollutants the SMPS.4 and
439 SMPS.6 are more enhanced. These variations are harder to distinguish using the OPC data, as
440 they are less apparent in the size range measured by the sensor. To further understand the
441 possible sources using the latter, information from other instrument which provide chemical

442 composition data are needed, though it is still hard to pinpoint exact sources, due to the OPC's
443 weakness in explaining distinct particle sources within the day.

444

445 **3.5 Case studies**

446

447 **OPC.2**

448 OPC.2 occurs mainly on a single day in March (12th) with higher than average temperature
449 and strong western winds. This was the cluster with the lowest concentrations of NH₄⁺, NO₃⁻
450 (about an order of magnitude compared to average conditions) and SO₄²⁻, rather low
451 concentrations of NO₂, BC and high O₃, which is probably the result of the strong winds and
452 the very high PBL height assisting in the removal of the pollutants from the site. Using the
453 SMPS data, this group of hours seems to follow the trends of BC, associating it with SMPS.6
454 for low, SMPS.1 and SMPS.2 for medium and SMPS.4 for higher concentrations of BC. This
455 cluster has very low PM₁ and PM_{2.5} and near average PM₁₀ concentrations, probably
456 associating it with marine sources (due to the high wind speed). Due to this, it is not clearly
457 separated using the SMPS data, which does so for the hours of this group according to the
458 level of fresher pollutants, the variation of which is smaller in this type of environments. This
459 cluster seems to be the result of the change in the wind profile which greatly affected the
460 coarser particles at the site (figure S5).

461

462 **OPC.3**

463 The third cluster formed using the OPC data, was a rather small group of hours in late January
464 (25,27 and 28th), with the lowest average temperature, wind speed and PBL height compared
465 to the rest of the clusters. The wind direction profile for this group contains both western and
466 southern winds, the latter being associated with high concentrations of pollutants (as found
467 by the study of the SMPS data). The majority of the hours in this group (65%) were
468 characterised as freshly polluted when using the SMPS data, mainly associated with SMPS.2.
469 Unfortunately, data of NO₂, BC, O₃ and PM for this group were very scarce from regulatory-
470 grade instruments (due to instrument error – the results provided in table 2 for the OPC.3 are
471 only from 2 hours of data that were available from the regulatory grade instrument). The
472 ACSM data, which were available for the hours of this cluster pointed to marginally lower

473 than average values of organic content, nitrate and ammonium, while the sulphate
474 concentrations were rather high. Using the low-cost sensor data, it is found that this group
475 has the highest BC (data from this low-cost sensor is not included), and involatile component
476 of LDSA. This group also had the highest average particle concentration in the size range of
477 the OPC, which is in agreement with the highest PM concentrations in all ranges (PM₁, PM_{2.5},
478 PM₁₀), and is probably the result of the low wind speed and PBL height. As this is not visible
479 from the SMPS, the cluster associated with this group has nearly average particle
480 concentrations in the SMPS particle ranges. This group was not distinctively detected by the
481 SMPS due to presenting variation in larger sized particles, which can be one of the weaknesses
482 of studying the sources of such particles using SMPS data alone. The OPC.3 appears to contain
483 the more polluted slow-moving portion of SMPS.2 with enhanced SO₄²⁻, BC and PM
484 concentrations.

485

486 **SMPS.3**

487 The third cluster from the analysis of SMPS data presented a unique profile with two peaks,
488 one below 30 nm and one a bit over 100 nm. This unique group was associated with very
489 clean conditions, with very low concentrations for all the pollutants with available data (apart
490 from O₃), as well as low particle concentrations for all the ranges in the SMPS and OPC range
491 as well as PM₁ and PM_{2.5}. The concentrations of PM₁₀ and SO₄²⁻ were somehow higher but
492 still lower than the average in the area for the period of the study. This group is associated
493 with high average temperature and wind speed and rather low RH, with wind directions being
494 mainly southwestern and western. This group occurred solely at night hours during a number
495 of relatively warm nights mainly in February and to a lesser extend in March. Even with very
496 low particle concentrations (as found by both the SMPS and OPC) the presence of two
497 separate peaks in the size range of the ultrafine particles is indicative of more than one
498 simultaneous source. Due to these sources of particles occurring at the ultrafine particle
499 range, the OPC was not able to distinguish this special condition and grouped the hours of
500 this cluster to a number of clusters (mainly OPC.5 and to a lesser extend OPC.1 and OPC.6),
501 occurring either during night-time or throughout the day. The inability of the OPC to
502 distinguish complicated conditions in the ultrafine range is a weakness of the OPC that should
503 be considered when such conditions are anticipated.

504

505 **4. Discussion**

506

507 As the SMPS measures smaller particle sizes and with better accuracy, compared to the OPC,
508 it managed to better separate the different sources of fresher pollution with the main
509 differentiating factor being the time of the day, for which the variability of such sources is
510 more prominent. The differences in NO₂ concentrations, which are mainly associated with
511 fresher emissions are more distinct between the groups and using this data better separation
512 of very clean (SMPS.3) and very polluted conditions from a distinct source (SMPS.5) was
513 achieved, while the other groups described mostly average conditions with lesser variability
514 (as expected in this range at a background site). Additionally, using the SMPS data it is possible
515 to distinguish multiple sources of ultrafine particles (SMPS.3), as they can appear as multiple
516 peaks within the SMPS spectra. This is not possible using the OPC data as the size range
517 measured by this instrument cannot identify such cases.

518 Contrary to the SMPS, using the OPC data provided less distinct separation of fresher
519 emissions (as expected due to the lack of data of small sized particles). Additionally, the OPC
520 data is less sensitive to diurnal variations due to the range of particles covered, which are in
521 a size range that does not vary significantly through the day but between days. This results in
522 the less distinct diurnal variations found between the groups formed. The analysis of the OPC
523 data though managed to adequately separate conditions and/or sources associated with
524 larger particles, such as aged pollution (for which it also managed to separate a small time-
525 window with very strong sulphate presence – OPC.3) which has the greatest contribution in
526 the particle chemical composition for the study area (Harrison et al., 2003; Taiwo, 2016; Yin
527 et al., 2010), RH variations or air masses of marine origin. To an extent, this might be due to
528 the number of clusters chosen as there is a possibility that a larger number of clusters from
529 the SMPS may separate sources of larger particles better, though with the risk of also
530 separating similar sources. Additionally, the pollution levels of the clusters formed directly
531 follow the trends of the PBL height in the area, a variation captured by both instruments,
532 showing the importance of this variable in the air quality of an area.

533 To sum up, the study of SMPS data with k-means clustering is far superior at separating
534 complex pollution sources within urban environments in which the variation of very small

535 particles is crucial for identifying particle and emission sources. This advantage of the SMPS
536 will not be overcome even with a denser measuring network of OPCs that could be acquired
537 for the same cost of the SMPS. However, clustering of the OPC data can provide useful
538 information to assess the sources of air pollution at background sites in which the direct
539 (smaller) particle sources are few. The method managed to find sources of greater pollution
540 associated with higher concentrations of particles of greater sizes (which are mainly
541 associated with aged pollution though), showing that the footprint of pollution in the ultrafine
542 particle range can have a detectable effect in coarser particle distributions as well. While not
543 as precise as the SMPS, a denser network of such instruments in background sites can be
544 more beneficial and more cost efficient in studying multiple pollution sources or “hot spots”
545 within the urban environment.

546 The current inability of low-cost PM sensors in measuring particle size spectra at small sizes
547 (<300 nm) is the greatest drawback in their application for separating particle sources, since
548 much information is contained in these smaller sizes. OPCs using shorter wavelength light
549 sources and hence smaller particle detection could be beneficial here. Also, there are several
550 low-cost sensors that provide insight for the surface area or the total number of particles in
551 the ultrafine particle size range (such as the LDSA sensor used in this study). The combined
552 use of the OPC with these instruments, along with sophisticated statistical techniques, may
553 provide possibilities for more precise source differentiation than shown in the present study.
554 It is noted that while clustering of particle number size distributions is one approach in the
555 study of the source assessment of particles, other alternative methods, such as the Positive
556 Matrix Factorisation (PMF), may also provide useful results.

557

558 **5. Conclusions**

559

560 The present study investigates the capabilities of a low-cost OPC sensor for source
561 differentiation at an urban background site in Birmingham, UK. It is used alongside a
562 regulatory-grade SMPS instrument, which has previously been used successfully for source
563 differentiation. The clustering approach identified optimal solutions of six clusters for both
564 the SMPS and OPC data. There were similarities between the SMPS and OPC solutions, which
565 provide insights into periods of low and high pollution. However, large differences were also

566 observed. A more distinct separation of direct emission sources was achieved using the SMPS
567 data, which identified sources with time windows that correlated with extreme NO₂
568 concentrations (either high or low), as well as periods with more complex sources. The OPC
569 was able to distinguish time periods with greater variation of super micron sized particle
570 sources (e.g. marine sources). There seems to be a clearer distinction of the diurnal variability
571 of sources using the SMPS data, while the OPC seems to be able to only distinguish the
572 variability within periods of days rather than hours, as found by the less variable diurnal and
573 weekly variation. This though might not be a great drawback when considering background
574 sites, as this variability is smaller in such environments which are mainly affected by regional
575 pollution, while the local emissions are less and more distinct. Low-cost sensors can be a
576 reliable alternative for source identification studies in environments with less complex
577 sources, which present smaller alterations within the span of the day. Still, such instruments
578 cannot be used for scientific analyses which require greater precision. Their application will
579 probably be adequate when studying the sources of particles with a more regional character
580 (e.g. marine sources) rather than direct and variable sources (e.g. traffic or cooking emissions)
581 and can provide enough information for the air quality levels, sources and conditions these
582 are anticipated from. Such studies may include the analysis of mineral dust events resulting
583 from either anthropogenic activities or meteorological events (e.g. dust storms), bioaerosol
584 events in forested areas and other sources which affect mainly the composition of coarser
585 particles.

586 This study demonstrates that single low-cost sensor PM units can provide sensible source
587 differentiation of large sized PM pollution sources. This allows for the prospect of source
588 apportionment via networks of low-cost sensors in the near future, thereby allowing
589 triangulation of sources. The development of more sophisticated low-cost sensors in
590 conjunction with their low cost ensures the prospect of the application of a denser
591 measurement network, making better air quality monitoring and control feasible in the near
592 future. This though, requires more similar studies which can further elucidate the strengths
593 and weaknesses of those sensors compared to the regulatory-grade ones, as they develop.

594

595 **Author Contributions**

596 The study was conceived and planned by FDP who also contributed to the final manuscript,
597 and DB who also carried out the analysis and prepared the first draft. AS, MH, DCSB and SD
598 have provided with the data for the analysis. DCSB provided help with the analysis of the
599 data. RMH provided advice on the analysis. PME and AB contributed to the final manuscript.

600

601 **Competing Interests**

602 The authors have no conflict of interests.

603

604 **Acknowledgements**

605 The work is funded by NERC (NE/T001879/1) and EPSRC (EP/T030100/1). We thank the OSCA
606 team at the Birmingham Air Quality Supersite (BAQS), funded by NERC (NE/T001909/1), for
607 help in data collection for the regulatory grade instruments. We thank Lee Chapman for
608 access to his meteorological data set used in the analysis.

609 **References**

610 Alam, A., Shi, J. P. and Harrison, R. M.: Observations of new particle formation in urban air, *J.*
611 *Geophys. Res. Atmos.*, 108(D3), 4093, doi:10.1029/2001JD001417, 2003.

612

613 Alam, M. S., Keyte, I. J., Yin, J., Stark, C., Jones, A. M. and Harrison, R. M.: Diurnal variability of
614 polycyclic aromatic compound (PAC) concentrations: Relationship with meteorological
615 conditions and inferred sources, *Atmos. Environ.*, 122, 427–438,
616 doi:10.1016/j.atmosenv.2015.09.050, 2015.

617

618 Alphasense User Manual for OPC-N3 Optical Particle Counter, Alphasense Ltd., 072-0502, pp.
619 32, Essex, UK, 2019.

620

621 Amegah, A. K.: Proliferation of low-cost sensors. What prospects for air pollution
622 epidemiologic research in Sub-Saharan Africa?, *Environ. Pollut.*, 241, 1132–1137,
623 doi:10.1016/j.envpol.2018.06.044, 2018.

624

625 Austin, E., Novoselov, I., Seto, E. and Yost, M. G.: Laboratory evaluation of the Shinyei
626 PPD42NS low-cost particulate matter sensor, *PLoS One*, 10(9), 1–17,
627 doi:10.1371/journal.pone.0137789, 2015.

628

629 Beddows, D. C. S., Dall’Osto, M. and Harrison, R. M.: Cluster analysis of rural, urban, and
630 curbside atmospheric particle size data, *Environ. Sci. Technol.*, 43(13), 4694–4700,
631 doi:10.1021/es803121t, 2009.

632

633 Beddows, D. C. S., Harrison, R. M., Green, D. C. and Fuller, G. W.: Receptor modelling of both
634 particle composition and size distribution from a background site in London, UK, *Atmos.*
635 *Chem. Phys.*, 15(17), 10107–10125, doi:10.5194/acp-15-10107-2015, 2015.

636

637 Von Bismarck-Osten, C. and Weber, S.: A uniform classification of aerosol signature size
638 distributions based on regression-guided and observational cluster analysis, *Atmos. Environ.*,
639 89, 346–357, doi:10.1016/j.atmosenv.2014.02.050, 2014.

640
641 Borrego, C., Ginja, J., Coutinho, M., Ribeiro, C., Karatzas, K., Sioumis, T., Katsifarakis, N.,
642 Konstantinidis, K., De Vito, S., Esposito, E., Salvato, M., Smith, P., André, N., Gérard, P., Francis,
643 L. A., Castell, N., Schneider, P., Viana, M., Minguillón, M. C., Reimringer, W., Otjes, R. P., von
644 Sicard, O., Pohle, R., Elen, B., Suriano, D., Pfister, V., Prato, M., Dipinto, S. and Penza, M.:
645 Assessment of air quality microsensors versus reference methods: The EuNetAir Joint Exercise
646 – Part II, *Atmos. Environ.*, 193, 127–142, doi:10.1016/j.atmosenv.2018.08.028, 2018.
647
648 Bousiotis, D., Brean, J., Pope, F.D., Dall'Osto, M., Querol, X., Alastuey, A., Perez, N., Petäjä,
649 T., Massling, A., Nøjgaard, J.K., Nordstrøm, C., Kouvarakis, G., Vratolis, S., Eleftheriadis, K.,
650 Niemi, J.V., Portin, H., Wiedensohler, A., Weinhold, K., Merkel, M., Tuch, T. and Harrison,
651 R.M.: The effect of meteorological conditions and atmospheric composition in the
652 occurrence and development of new particle formation (NPF) events in Europe, *Atmos.*
653 *Chem. Phys.*, 21(5), 3345 - 3370, <https://doi.org/10.5194/acp-21-3345-2021>, 2021.
654
655 Bousiotis, D., Dall'Osto, M., Beddows, D. C. S., Pope, F. D., Harrison, R. M. and Harrison, C. R.
656 M.: Analysis of new particle formation (NPF) events at nearby rural , urban background and
657 urban roadside sites, 5679–5694, 2019.
658
659 Brines, M., Dall'Osto, M., Beddows, D.C.S., Harrison, R.M., Gomez-Moreno, F., Nuñez, L.,
660 Artiñano, B., Costabile, F., Gobbi, G.P., Salimi, F., Morawska, L., Sioutas, C. and Querol, X.:
661 Traffic and nucleation events as main sources of ultrafine particles in high-insolation
662 developed world cities, *Atmos. Chem. Phys.*, 15, 5929 - 5945, <https://doi.org/10.5194/acp-15-5929-2015>, 2015.
664
665 Carslaw, D. C. and Ropkins, K.: openair — An R package for air quality data analysis, *Environ.*
666 *Model. Softw.*, 27–28, 52–61, doi:10.1016/j.envsoft.2011.09.008, 2012.
667
668 Castell, N., Dauge, F. R., Schneider, P., Vogt, M., Lerner, U., Fishbain, B., Broday, D. and
669 Bartonova, A.: Can commercial low-cost sensor platforms contribute to air quality monitoring
670 and exposure estimates?, *Environ. Int.*, 99, 293–302, doi:10.1016/j.envint.2016.12.007, 2017.
671

672 Crilley, L. R., Singh, A., Kramer, L. J., Shaw, M. D., Alam, M. S., Apte, J. S., Bloss, W. J.,
673 Hildebrandt Ruiz, L., Fu, P., Fu, W., Gani, S., Gatari, M., Ilyinskaya, E., Lewis, A. C., Ng'ang'a,
674 D., Sun, Y., Whitty, R. C. W., Yue, S., Young, S. and Pope, F. D.: Effect of aerosol composition
675 on the performance of low-cost optical particle counter correction factors, *Atmos. Meas. Tech.*, 13(3), 1181–1193, doi:10.5194/amt-13-1181-2020, 2020.

677

678 Crilley, L.R., Shaw, M., Pound, R., Kramer, L.J., Price, R., Young, S., Lewis, A.C. and Pope F.D.:
679 Evaluation of a low-cost optical particle counter (Alphasense OPC-N2) for ambient
680 monitoring, *Atmos. Meas. Tech.*, 11(2), 709 - 720, <https://doi.org/10.5194/amt-11-709-2018>.

682

683 Dall'Osto, M., Beddows, D.C.S, Pey, J., Rodriguez, S., Alastuey, A., Harrison, R.M., and
684 Querol, X.: Urban aerosol size distributions over the Mediterannean city of Barcelona, NE
685 Spain, *Atmos. Chem. Phys.*, 12, 10693 - 10707, <https://doi.org/10.5194/acp-12-10693-2012>,
686 2012.

687

688 Dall'Osto, M., Monahan, C., Greaney, R., Beddows, D. C. S., Harrison, R. M., Ceburnis, D. and
689 O'Dowd, C. D.: A statistical analysis of North East Atlantic (submicron) aerosol size
690 distributions, *Atmos. Chem. Phys.*, 11(24), 12567–12578, doi:10.5194/acp-11-12567-2011,
691 2011.

692

693 Di Antonio, A., Popoola, O. A. M., Ouyang, B., Saffell, J and Jones, R. L.: Developing a relative
694 humidity correction for low-cost sensors measuring ambient particulate matter, *Sensors*
695 (Switzerland), 18(9). <https://doi.org/10.3390/s18092790>, 2018.

696

697 Dockery, D. W., Pope III, C. A., Xu, X., Spengler, J. D., Ware, J. H., Fay, M. E., G., F. B. and E., S.
698 F.: An association between air pollution and mortality in six U.S. cities, *N. Engl. J. Med.*,
699 329(24), 1753–1759, 1993.

700

701 Draxler, R. R. and Hess, G. D.: An Overview of the HYSPLIT_4 Modelling System for
702 Trajectories, Dispersion, and Deposition, *Aust. Meteorol. Mag.*, 47(January), 295–308, 1998.

703 Feinberg, S. N., Williams, R., Hagler, G., Low, J., Smith, L., Brown, R., Garver, D., Davis, M.,

704 Morton, M., Schaefer, J. and Campbell, J.: Examining spatiotemporal variability of urban
705 particulate matter and application of high-time resolution data from a network of low-cost
706 air pollution sensors, *Atmos. Environ.*, 213(May), 579–584,
707 doi:10.1016/j.atmosenv.2019.06.026, 2019.

708

709 Ghosh, D. and Parida, P.: Air Pollution and India: Current Scenario, *Int. J. Curr. Res.*, 7(11),
710 22194–22196, 2015.

711

712 Giorio, C., Tapparo, A., Dallusto, M., Beddows, D. C. S., Esser-Gietl, J. K., Healy, R. M. and
713 Harrison, R. M.: Local and regional components of aerosol in a heavily trafficked street canyon
714 in central London derived from PMF and cluster analysis of single-particle ATOFMS spectra,
715 *Environ. Sci. Technol.*, 49(6), 3330–3340, doi:10.1021/es506249z, 2015.

716

717 Hagan, D.H., Kroll, J.H., Assessing the accuracy of low-cost optical particle sensors using a
718 physics-based approach, *Atmos. Meas. Tech.*, 13, 6343 - 6355, 2020.

719

720 Hagan, D. H., Gani, S., Bhandari, S., Patel, K., Habib, G., Apte, J. S., Hildebrandt Ruiz, L. and
721 Kroll, J. H.: Inferring Aerosol Sources from Low-Cost Air Quality Sensor Measurements: A Case
722 Study in Delhi, India, *Environ. Sci. Technol. Lett.*, 6(8), 467–472,
723 doi:10.1021/acs.estlett.9b00393, 2019.

724

725 Harrison, R. M.: Urban atmospheric chemistry: a very special case for study, *npj Clim. Atmos.*
726 *Sci.*, 1(1), 5, doi:10.1038/s41612-017-0010-8, 2017.

727

728 Harrison, R. M., Deacon, A. R., Jones, M. R. and Appleby, R. S.: Sources and processes affecting
729 concentrations of PM10 and PM2.5 particulate matter in Birmingham (U.K.), *Atmos. Environ.*,
730 31(24), 4103–4117, doi:10.1016/S1352-2310(97)00296-3, 1997.

731

732 Harrison, R. M., Jones, A. M. and Lawrence, R. G.: A pragmatic mass closure model for airborne
733 particulate matter at urban background and roadside sites, *Atmos. Environ.*, 37(35), 4927–
734 4933, doi:10.1016/j.atmosenv.2003.08.025, 2003.

735

736 Harrison, R. M., Jones, A. M. and Lawrence, R. G.: Major component composition of PM10
737 and PM2.5 from roadside and urban background sites, *Atmos. Environ.*, 38(27), 4531–4538,
738 doi:10.1016/j.atmosenv.2004.05.022, 2004.

739

740 Holstius, D. M., Pillarisetti, A., Smith, K. R. and Seto, E.: Field calibrations of a low-cost aerosol
741 sensor at a regulatory monitoring site in California, *Atmos. Meas. Tech.*, 7(4), 1121–1131,
742 doi:10.5194/amt-7-1121-2014, 2014.

743

744 Ionascu, M. E., Gruicin, I. and Marcu, M.: Laboratory evaluation and calibration of low-cost
745 sensors for air quality measurement, *SACI 2018 - IEEE 12th Int. Symp. Appl. Comput. Intell.*
746 *Informatics, Proc.*, 395–400, doi:10.1109/SACI.2018.8440974, 2018.

747

748 Jerrett, M., Donaire-Gonzalez, D., Popoola, O., Jones, R., Cohen, R. C., Almanza, E., de Nazelle,
749 A., Mead, I., Carrasco-Turigas, G., Cole-Hunter, T., Triguero-Mas, M., Seto, E. and
750 Nieuwenhuijsen, M.: Validating novel air pollution sensors to improve exposure estimates for
751 epidemiological analyses and citizen science, *Environ. Res.*, 158(April), 286–294,
752 doi:10.1016/j.envres.2017.04.023, 2017.

753

754 Jovašević-Stojanović, M., Bartonova, A., Topalović, D., Lazović, I., Pokrić, B. and Ristovski, Z.:
755 On the use of small and cheaper sensors and devices for indicative citizen-based monitoring
756 of respirable particulate matter, *Environ. Pollut.*, 206, 696–704,
757 doi:10.1016/j.envpol.2015.08.035, 2015.

758

759 Kan, H., Chen, B. and Hong, C.: Health impact of outdoor air pollution in China: Current
760 knowledge and future research needs, *Environ. Health Perspect.*, 117(5), 12737,
761 doi:10.1289/ehp.12737, 2009.

762

763 Kanaroglou, P. S., Jerrett, M., Morrison, J., Beckerman, B., Arain, M. A., Gilbert, N. L. and
764 Brook, J. R.: Establishing an air pollution monitoring network for intra-urban population
765 exposure assessment: A location-allocation approach, *Atmos. Environ.*, 39(13), 2399–2409,
766 doi:10.1016/j.atmosenv.2004.06.049, 2005.

767

768 Kelly, K. E., Whitaker, J., Petty, A., Widmer, C., Dybwad, A., Sleeth, D., Martin, R. and
769 Butterfield, A.: Ambient and laboratory evaluation of a low-cost particulate matter sensor,
770 Environ. Pollut., 221, 491–500, doi:10.1016/j.envpol.2016.12.039, 2017.

771

772 Kotsev, A., Schade, S., Craglia, M., Gerboles, M., Spinelle, L. and Signorini, M.: Next generation
773 air quality platform: Openness and interoperability for the internet of things, Sensors
774 (Switzerland), 16(3), doi:10.3390/s16030403, 2016.

775

776 Kumar, P., Morawska, L., Martani, C., Biskos, G., Neophytou, M., Di Sabatino, S., Bell, M.,
777 Norford, L. and Britter, R.: The rise of low-cost sensing for managing air pollution in cities,
778 Environ. Int., 75, 199–205, doi:10.1016/j.envint.2014.11.019, 2015.

779

780 Lagerspetz, E., Motlagh, N. H., Arbayani Zaidan, M., Fung, P. L., Mineraud, J., Varjonen, S.,
781 Siekkinen, M., Nurmi, P., Matsumi, Y., Tarkoma, S. and Hussein, T.: MegaSense: Feasibility of
782 Low-Cost Sensors for Pollution Hot-spot Detection, IEEE Int. Conf. Ind. Informatics, 2019-July,
783 1083–1090, doi:10.1109/INDIN41052.2019.8971963, 2019.

784

785 Lewis, A. C., von Schneidemesser, E., Peltier, R. E., Lung, C., Jones, R., Zellweger, C., Karppinen,
786 A., Penza, M., Dye, T., Hüglin, C., Ning, Z., Leigh, R., Hagan, D. H., Laurent, O. and Carmichael,
787 G.: Low-cost sensors for the measurement of atmospheric composition: overview of topic and
788 future applications. [online] Available from:
789 http://www.wmo.int/pages/prog/arep/gaw/documents/Draft_low_cost_sensors.pdf, 2018.

790

791 Likas, A., Vlassis, N. and Verbeek, J.J.: The global k-means clustering algorithm, Pattern
792 Recognition, 36(2), 451-461, [https://doi.org/10.1016/S0031-3203\(02\)00060-2](https://doi.org/10.1016/S0031-3203(02)00060-2), 2003.

793

794 Mahbub, P., Ayoko, G.A., Goonetilleke, A., Egodawatta, P.: Analysis of the build-up of semi
795 and non volatile organic compounds on urban roads, Water Res. 45(9), 2835 - 2844, doi:
796 10.1016/j.watres.2011.02.033, 2011.

797

798 Malings, C., Tanzer, R., Hauryliuk, A., Saha, P. K., Robinson, A. L., Presto, A. A. and
799 Subramanian, R.: Fine particle mass monitoring with low-cost sensors: Corrections and long-
800 term performance evaluation, Aerosol Sci. Technol., 54(2), 160–174,

801 doi:10.1080/02786826.2019.1623863, 2020.

802

803 McGregor, G.R., Bamzelis, D.: Synoptic typing and its application to the investigation of
804 weather air pollution relationships, Birmingham, United Kingdom, Theoretical and Applied
805 Climatology, 51, 223 - 236, 1995.

806

807 Miskell, G., Salmond, J. and Williams, D. E.: Low-cost sensors and crowd-sourced data:
808 Observations of siting impacts on a network of air-quality instruments, Sci. Total Environ.,
809 575, 1119–1129, doi:10.1016/j.scitotenv.2016.09.177, 2017.

810

811 Miskell, G., Salmond, J. A. and Williams, D. E.: Use of a handheld low-cost sensor to explore
812 the effect of urban design features on local-scale spatial and temporal air quality variability,
813 Sci. Total Environ., 619–620, 480–490, doi:10.1016/j.scitotenv.2017.11.024, 2018.

814

815 Moltchanov, S., Levy, I., Etzion, Y., Lerner, U., Broday, D. M. and Fishbain, B.: On the feasibility
816 of measuring urban air pollution by wireless distributed sensor networks, Sci. Total Environ.,
817 502, 537–547, doi:10.1016/j.scitotenv.2014.09.059, 2015.

818

819 Morawska, L., Thai, P.K., Liu, X., Asumadu-Sakyi, A., Ayoko, G., Bartonova, A., Bedini, A., Chai,
820 F., Christensen, B., Dunbabin, M., Gao, J., Hagler, G.S.W., Jayaratne, R., Kumar, M., Lau, A.K.H.,
821 Louie, P.K.K., Mazaheri, M., Ning, Z., Motta, N., Mullins, B., Rahman, M.M., Ristovski, Z.,
822 Shafiei, M., Tjondronegoro, D., Westerdahl, D. and Williams, R.: Applications of low-
823 costsensing technologies for a quality air monitoring and exposure assessment: How far have
824 they gone?, Environment International, 116, 286 - 299,
825 https://doi.org/10.1016/j.envint.2018.04.018, 2018.

826

827 Mueller, M. D., Hasenfratz, D., Saukh, O., Fierz, M. and Hueglin, C.: Statistical modelling of
828 particle number concentration in Zurich at high spatio-temporal resolution utilizing data from
829 a mobile sensor network, Atmos. Environ., 126, 171–181,
830 doi:10.1016/j.atmosenv.2015.11.033, 2016.

831

832 Nagendra, S., Reddy Yasa, P., Narayana, M., Khadirnaikar, S. and Pooja Rani: Mobile

833 monitoring of air pollution using low cost sensors to visualize spatio-temporal variation of
834 pollutants at urban hotspots, *Sustain. Cities Soc.*, 44(September 2018), 520–535,
835 doi:10.1016/j.scs.2018.10.006, 2019.

836

837 Pakhira, M.K., Bandyopadhyay, S. and Maulik, U.: Validity index of crisp and fuzzy clusters,
838 *Pattern Recognition*, 37(3), 487-501, <https://doi.org/10.1016/j.patcog.2003.06.005>, 2004.

839

840 Pascal, M., Corso, M., Chanel, O., Declercq, C., Badaloni, C., Cesaroni, G., Henschel, S., Meister,
841 K., Haluza, D., Martin-Olmedo, P. and Medina, S.: Assessing the public health impacts of urban
842 air pollution in 25 European cities: Results of the Aphekom project, *Sci. Total Environ.*,
843 449(2007105), 390–400, doi:10.1016/j.scitotenv.2013.01.077, 2013.

844

845 Penza, M., Suriano, D., Villani, M. G., Spinelle, L. and Gerboles, M.: Towards air quality indices
846 in smart cities by calibrated low-cost sensors applied to networks, in *Proceedings of IEEE
847 Sensors*, vol. 2014-Decem, pp. 2012–2017., 2014.

848

849 Petkova, E. P., Jack, D. W., Volavka-Close, N. H. and Kinney, P. L.: Particulate matter pollution
850 in African cities, *Air Qual. Atmos. Heal.*, 6(3), 603–614, doi:10.1007/s11869-013-0199-6, 2013.

851

852 Pope, F. D., Gatari, M., Ng'ang'a, D., Poynter, A. and Blake, R.: Airborne particulate matter
853 monitoring in Kenya using calibrated low cost sensors, *Atmos. Chem. Phys. Discuss.*, 1–31,
854 doi:10.5194/acp-2018-327, 2018.

855

856 Popoola, O. A. M., Carruthers, D., Lad, C., Bright, V. B., Mead, M. I., Stettler, M. E. J., Saffell, J.
857 R. and Jones, R. L.: Use of networks of low cost air quality sensors to quantify air quality in
858 urban settings, *Atmos. Environ.*, 194(February), 58–70, doi:10.1016/j.atmosenv.2018.09.030,
859 2018.

860

861 Rai, A. C., Kumar, P., Pilla, F., Skouloudis, A. N., Di Sabatino, S., Ratti, C., Yasar, A. and Rickerby,
862 D.: End-user perspective of low-cost sensors for outdoor air pollution monitoring, *Sci. Total
863 Environ.*, 607–608, 691–705, doi:10.1016/j.scitotenv.2017.06.266, 2017.

864

865 Rousseeuw, P.J.: Silhouettes: A graphical aid to the interpretation and validation of cluster
866 analysis, *Journal of Computational and Applied Mathematics*, 20, 53-65,
867 [https://doi.org/10.1016/0377-0427\(87\)90125-7](https://doi.org/10.1016/0377-0427(87)90125-7), 1987.

868

869 Sabaliauskas, K., Jeong, C.-H. H., Yao, X., Jun, Y.-S. S. and Evans, G.: Cluster analysis of roadside
870 ultrafine particle size distributions, *Atmos. Environ.*, 70(0), 64–74,
871 doi:<http://dx.doi.org/10.1016/j.atmosenv.2012.12.025>, 2013.

872

873 Salimi, F., Ristovski, Z., Mazaheri, M., Laiman, R., Crilley, L. R., He, C., Clifford, S. and
874 Morawska, L.: Assessment and application of clustering techniques to atmospheric particle
875 number size distribution for the purpose of source apportionment, *Atmos. Chem. Phys.*,
876 14(21), 11883–11892, doi:10.5194/acp-14-11883-2014, 2014.

877

878 Sayahi, T., Butterfield, A. and Kelly, K. E.: Long-term field evaluation of the Plantower PMS
879 low-cost particulate matter sensors, *Environ. Pollut.*, 245, 932–940,
880 doi:10.1016/j.envpol.2018.11.065, 2019.

881

882 Schneider, P., Castell, N., Vogt, M., Dauge, F. R., Lahoz, W. A. and Bartonova, A.: Mapping
883 urban air quality in near real-time using observations from low-cost sensors and model
884 information, *Environ. Int.*, 106(May), 234–247, doi:10.1016/j.envint.2017.05.005, 2017.

885

886 Shindler, L., Development of a low-cost sensing platform for air quality monitoring:
887 Application in the city of Rome, *Environmental Technology*, 42:4, 618 - 631,
888 doi:10.1080/09593330.2019.1640290, 2019.

889

890 Schnelle-Kreis, J., Sklorz, M., Orasche, J., Stölzel, M., Peters, A. and Zimmermann, R.: Semi
891 volatile organic compounds in ambient PM_{2.5}. Seasonal trends and daily resolved source
892 contributions, *Environ. Sci. Technol.*, 41(11), 3821–3828, doi:10.1021/es060666e, 2007.

893

894 Snyder, E. G., Watkins, T. H., Solomon, P. A., Thoma, E. D., Williams, R. W., Hagler, G. S. W.,
895 Shelow, D., Hindin, D. A., Kilaru, V. J. and Preuss, P. W.: The changing paradigm of air pollution
896 monitoring, *Environ. Sci. Technol.*, 47(20), 11369–11377, doi:10.1021/es4022602, 2013.

897

898 Sousan, S., Koehler, K., Thomas, G., Park, J. H., Hillman, M., Halterman, A. and Peters, T. M.:
899 Inter-comparison of low-cost sensors for measuring the mass concentration of occupational
900 aerosols, *Aerosol Sci. Technol.*, 50(5), 462–473, doi:10.1080/02786826.2016.1162901, 2016.

901

902 Spinelle, L., Gerboles, M., Villani, M. G., Aleixandre, M. and Bonavitacola, F.: Field calibration
903 of a cluster of low-cost available sensors for air quality monitoring. Part A: Ozone and nitrogen
904 dioxide, *Sensors Actuators, B Chem.*, 215, 249–257, doi:10.1016/j.snb.2015.03.031, 2015.

905

906 Spinelle, L., Gerboles, M., Villani, M. G., Aleixandre, M. and Bonavitacola, F.: Field calibration
907 of a cluster of low-cost commercially available sensors for air quality monitoring. Part B: NO,
908 CO and CO₂, *Sensors Actuators, B Chem.*, 238, 706–715, doi:10.1016/j.snb.2016.07.036,
909 2017.

910

911 Taiwo, A. M.: Source apportionment of urban background particulate matter in Birmingham,
912 United Kingdom using a mass closure model, *Aerosol Air Qual. Res.*, 16(5), 1244–1252,
913 doi:10.4209/aaqr.2015.09.0537, 2016.

914

915 Taiwo, A. M., Beddows, D. C. S., Shi, Z. and Harrison, R. M.: Mass and number size distributions
916 of particulate matter components: Comparison of an industrial site and an urban background
917 site, *Sci. Total Environ.*, 475, 29–38, doi:10.1016/j.scitotenv.2013.12.076, 2014.

918

919 U.S. Environmental Protection Agency: Quality Assurance Guidance Document 2.12, , 105
920 [online] Available from: <https://www3.epa.gov/ttnamti1/files/ambient/pm25/qa/m212.pdf>,
921 2016.

922

923 United States Environmental Protection Agency: The National Ambient Air Quality Standards
924 for Particle Matter: Revised Air Quality Standards for Particle Pollution and Updates to the Air
925 Quality Index (AQI), Environ. Prot. Agency, 1–5 [online] Available from:
926 <http://www.epa.gov/pm/2012/declsstandards.pdf>, 2012.

927

928 Wang, Y., Li, J., Jing, H., Zhang, Q., Jiang, J. and Biswas, P.: Laboratory Evaluation and

929 Calibration of Three Low-Cost Particle Sensors for Particulate Matter Measurement, *Aerosol*
930 *Sci. Technol.*, 49(11), 1063–1077, doi:10.1080/02786826.2015.1100710, 2015.

931

932 Wegner, T., Hussein, T., Hämeri, K., Vesala, T., Kulmala, M. and Weber, S.: Properties of
933 aerosol signature size distributions in the urban environment as derived by cluster analysis,
934 *Atmos. Environ.*, 61, 350–360, doi:10.1016/j.atmosenv.2012.07.048, 2012.

935

936 Weyers, R., Jang-Jaccard, J., Moses, A., Wang, Y., Boulic, M., Chitty, C., Phipps, R. and
937 Cunningham, C.: Low-cost Indoor Air Quality (IAQ) Platform for Healthier Classrooms in New
938 Zealand: Engineering Issues, *Proc. - 2017 4th Asia-Pacific World Congr. Comput. Sci. Eng.*
939 APWC CSE 2017, (December), 208–215, doi:10.1109/APWConCSE.2017.00045, 2018.

940

941 World Health Organization: Air quality guidelines for particulate matter, ozone, nitrogen
942 dioxide and sulfur dioxide - Global update 2005., 2006.

943

944 Wu, S., Ni, Y., Li, H., Pan, L., Yang, D., Baccarelli, A. A., Deng, F., Chen, Y., Shima, M. and Guo,
945 X.: Short-term exposure to high ambient air pollution increases airway inflammation and
946 respiratory symptoms in chronic obstructive pulmonary disease patients in Beijing, China,
947 *Environ. Int.*, 94, 76–82, doi:10.1016/j.envint.2016.05.004, 2016.

948

949 Xu, Y., Zhang, J.S.: Understanding SVOCs, *ASHRAE Journal*, 53 (12), 121 - 125, 2011.

950

951 Yin, J., Harrison, R. M., Chen, Q., Rutter, A. and Schauer, J. J.: Source apportionment of fine
952 particles at urban background and rural sites in the UK atmosphere, *Atmos. Environ.*, 44(6),
953 841–851, doi:10.1016/j.atmosenv.2009.11.026, 2010.

954

955 Zeger, S. L., Dominici, F., McDermott, A. and Samet, J. M.: Mortality in the medicare
956 population and Chronic exposure to fine Particulate air pollution in urban centers (2000-
957 2005), *Environ. Health Perspect.*, 116(12), 1614–1619, doi:10.1289/ehp.11449, 2008.

958

959 Zheng, T., Bergin, M. H., Johnson, K. K., Tripathi, S. N., Shirodkar, S., Landis, M. S., Sutaria, R.
960 and Carlson, D. E.: Field evaluation of low-cost particulate matter sensors in high-and low-

961 concentration environments, *Atmos. Meas. Tech.*, 11(8), 4823–4846, doi:10.5194/amt-11-
962 4823-2018, 2018.

963

964

965 **TABLE LEGENDS**

966

967 **Table 1:** List of the measuring instruments used in the present study.

968

969 **Table 2:** Average atmospheric conditions for the clusters formed by both methods.

970

971 **Table 3:** Simultaneous occurrences of the clusters formed by both the OPC and SMPS.

972

973 **FIGURE LEGENDS**

974

975 **Figure 1:** Map of the location of the Birmingham Air Quality Supersite (BAQS) site in the
976 U.K. (Map by ©HERE).

977

978 **Figure 2:** Frequency and diurnal variation of the clusters formed by the OPC data.

979

980 **Figure 3:** Frequency and diurnal variation of the clusters formed by the SMPS data.

981

982 **Figure 4:** Particle contributions in the range 12 – 550 nm (using the SMPS data), for the
983 clusters formed using the OPC data (top) and the SMPS data (bottom).

984

985 **Figure 5:** Particle contributions in the range up to 10 μm (using the FIDAS data), for the
986 clusters formed using the OPC data (top) and the SMPS data (bottom).

987

988 **Figure 6:** Polar plots for the PM_1 ($\mu\text{g m}^{-3}$) for the clusters formed by the OPC data.

989

990 **Figure 7:** Weekly contribution (week number refers to week of year 2020) of the clusters
991 formed by the OPC (top) and SMPS (bottom).

992

993 **Table 1: List of the measuring instruments used in the present study.**

994

Monitoring	Model	Manufacturer	Regulatory grade	Approximate cost (£)
NO ₂	NO2-B43F	Alphasense	No	250
O _x	Ox-B43I	Alphasense	No	160
Black Carbon	MA200	Aethlabs	No	5,700
Lung Deposited Surface Area		Naneos	No	8,500
OPC	OPC-N3	Alphasense	No	250
SMPS	TSi3082	TSi	Yes	80,000
ACSM	Quad - ACSM	Aerodyne	Yes	170,000
PM	Fidas 200E	Palas	Yes	25,000
NO ₂	T500U	Teledyne	Yes	15,000
Black Carbon	AE33 Aethalometer	Magee Scientific	Yes	25,000
O ₃	49i	Thermo	Yes	3,000

995

996

Table 2: Average atmospheric conditions for the clusters formed by both methods.

	NO ₂ (ppb)	BC (ng m ⁻³)	PM ₁ (μg m ⁻³)	PM _{2.5} (μg m ⁻³)	PM ₁₀ (μg m ⁻³)	O ₃ (ppb)	Organic content (μg m ⁻³)	SO ₄ ²⁻ (μg m ⁻³)	NO ₃ ⁻ (μg m ⁻³)	LDSA ratio	RH (%)	WS (m s ⁻¹)	T (°C)	PBL height (m)
OPC.1	18.6±13.9	555±630	4.32±4.08	6.53±4.62	9.97±5.81	31.9±9.81	0.254±0.231	4.12E-02±5.42E-02	8.90E-02±1.15E-01	0.443	83.9±13.1	4.16±2.50	5.20±3.11	852±568
OPC.2	9.64±1.90	233±32.8	2.56±0.72	5.61±1.58	10.7±2.97	38.6±1.34	0.142±0.082	2.98E-02±5.67E-02	1.64E-02±5.53E-03	0.847	65.1±10.5	7.1±1.01	7.16±1.53	1622±264
OPC.3	13.1±8.20	278±153	2.95±0.78	5.80±1.98	9.70±2.69	37.6±6.79	0.241±0.254	6.73E-02±6.25E-02	8.41E-02±1.54E-01	0.830	91.8±8.73	3.47±1.11	4.60±1.95	732±312
OPC.4	11.5±7.15	281±191	2.51±1.55	4.84±3.20	8.33±5.35	36.5±5.17	0.192±0.235	4.53E-02±6.62E-02	1.08E-01±2.53E-01	0.536	83.5±11.5	4.37±2.09	6.26±2.73	930±430
OPC.5	18.3±16.3	659±879	6.27±6.56	9.10±7.18	13.3±8.37	31.5±11.9	0.338±0.558	4.10E-02±6.49E-02	1.31E-01±2.62E-01	0.417	82.6±11.5	4.38±2.50	6.68±3.31	835±485
OPC.6	8.58±6.72	197±155	2.85±1.12	5.96±2.51	10.3±4.30	40.0±4.69	0.116±0.152	3.50E-02±5.08E-02	3.50E-02±1.18E-01	0.588	81.2±12.3	4.87±2.07	6.42±2.89	1135±408
Average	15.9±13.7	498±673	4.53±4.93	7.11±5.61	11.0±6.94	33.6±9.95	0.252±0.403	4.19E-02±6.05E-02	1.00E-01±2.08E-01	0.499	83.1±12.3	4.37±2.37	6.05±3.11	901±504

	NO ₂ (ppb)	BC (ng m ⁻³)	PM ₁ (μg m ⁻³)	PM _{2.5} (μg m ⁻³)	PM ₁₀ (μg m ⁻³)	O ₃ (ppb)	Organic content (μg m ⁻³)	SO ₄ ²⁻ (μg m ⁻³)	NO ₃ ⁻ (μg m ⁻³)	LDSA ratio	RH (%)	WS (m s ⁻¹)	T (°C)	PBL height (m)
SMPS.1	16.0±14.9	485±852	3.35±2.64	5.70±3.89	9.52±6.05	32.2±10.3	0.215±0.300	3.06E-02±4.80E-02	5.47E-02±7.76E-02	0.331	85.1±10.7	4.1±2.70	5.53±3.06	771±558
SMPS.2	16.8±12.0	406±539	2.70±1.57	5.11±2.33	8.91±3.75	32.9±8.10	0.132±0.156	2.53E-02±4.11E-02	2.56E-02±4.31E-02	0.501	83.2±9.71	3.74±1.67	4.64±2.86	831±441
SMPS.3	4.38±2.91	88.1±62.2	2.64±1.62	5.57±3.62	9.26±5.87	41.6±3.24	0.062±0.063	3.74E-02±5.75E-02	2.07E-02±7.15E-02	0.555	80.1±8.93	7.19±2.48	7.43±2.72	1378±290
SMPS.4	14.3±12.3	452±592	3.77±2.56	6.71±3.75	11.1±5.67	35.6±9.32	0.249±0.306	4.68E-02±6.27E-02	8.12E-02±1.53E-01	0.499	79.4±13.9	4.74±2.38	6.97±2.62	1022±540
SMPS.5	29.8±17.2	1389±838	17.95±7.89	21.1±8.08	25.1±7.95	16.1±10.6	1.066±0.562	1.41E-01±7.58E-02	5.74E-01±3.60E-01	0.833	93.9±7.49	2.6±1.63	4.90±2.94	454±330
SMPS.6	13.2±10.8	340±395	2.68±1.58	5.23±3.12	9.12±5.42	36.0±6.54	0.164±0.189	2.93E-02±4.31E-02	3.86E-02±7.17E-02	0.467	81.0±12.7	4.73±2.11	6.1±3.11	1092±426
Average	15.1±13.2	460±649	4.12±4.72	6.78±5.48	10.8±6.90	33.8±9.84	0.280±0.403	4.61E-02±6.40E-02	1.07E-02±2.23E-01	0.499	82.8±12.4	4.41±2.42	5.95±2.99	929±517

Table 3: Simultaneous occurrences of the clusters formed by both the OPC and SMPS.

OPC/SMPS	SMPS.1	SMPS.2	SMPS.3	SMPS.4	SMPS.5	SMPS.6	Total OPC
OPC.1	48	30	9	71	13	66	237
OPC.2	1	3		5		3	12
OPC.3		15		2	4	2	23
OPC.4	25	27	6	52	19	50	179
OPC.5	24	26	17	39	40	38	184
OPC.6	7	25	9	28	3	25	97
Total SMPS	105	126	41	197	79	184	732



Figure 1: Map of the location of the Birmingham Air Quality Supersite (BAQS) site in the U.K. (Map by ©HERE).

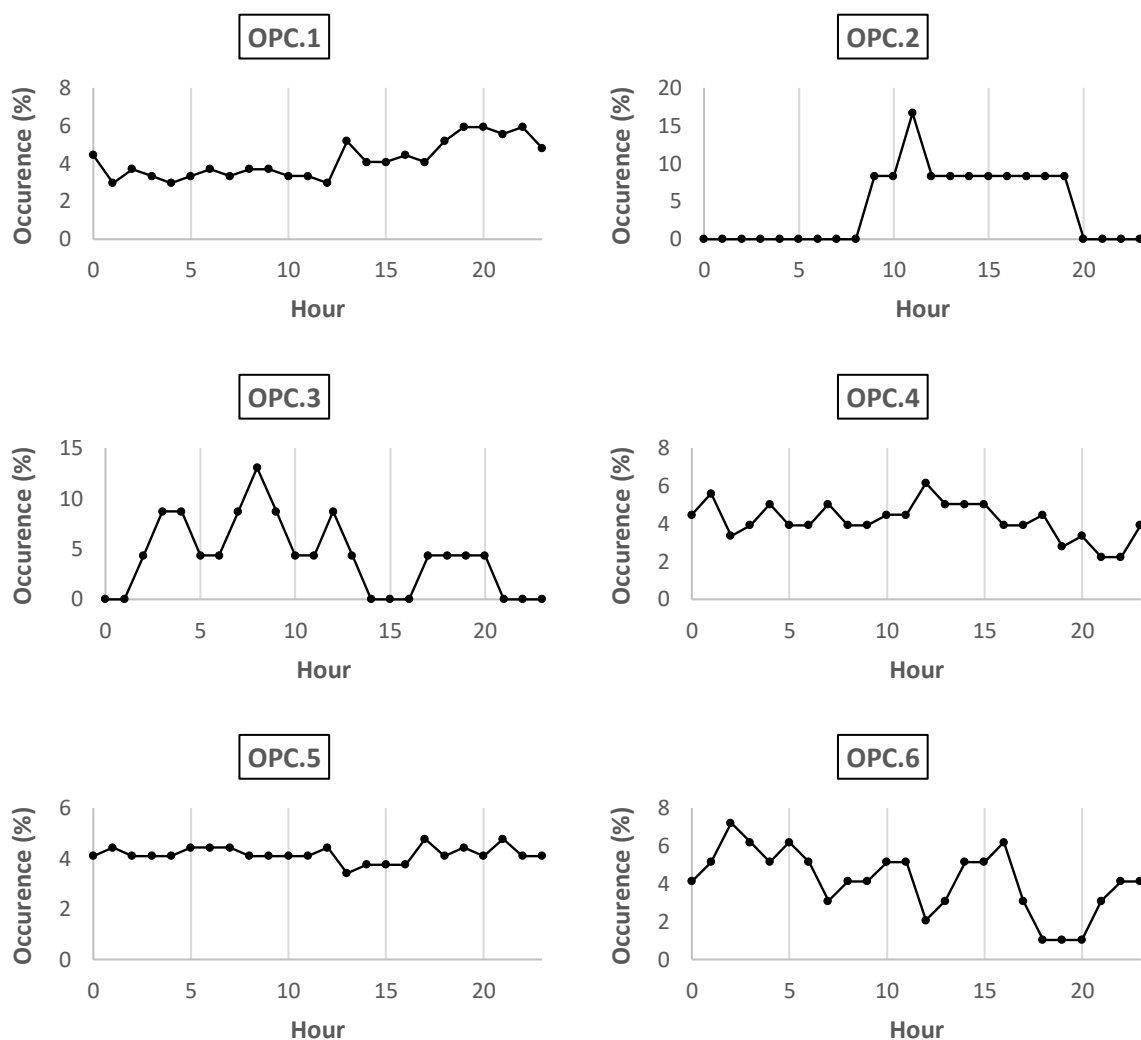
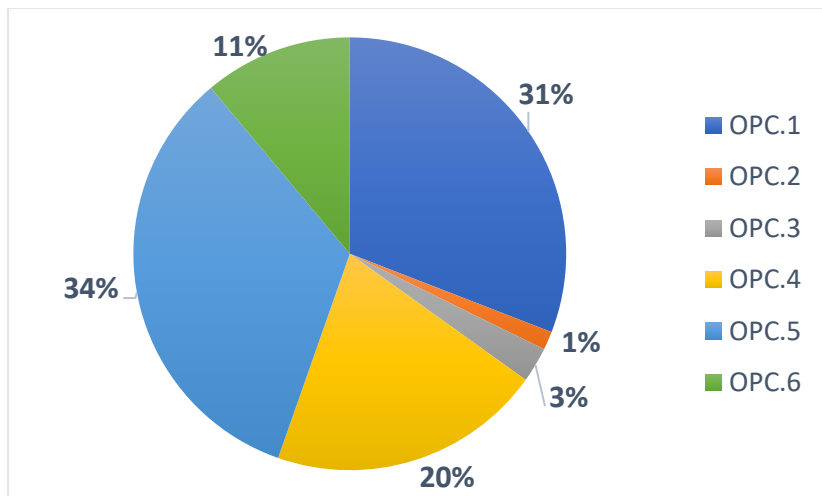


Figure 2: Frequency and diurnal variation of the clusters formed by the OPC data.

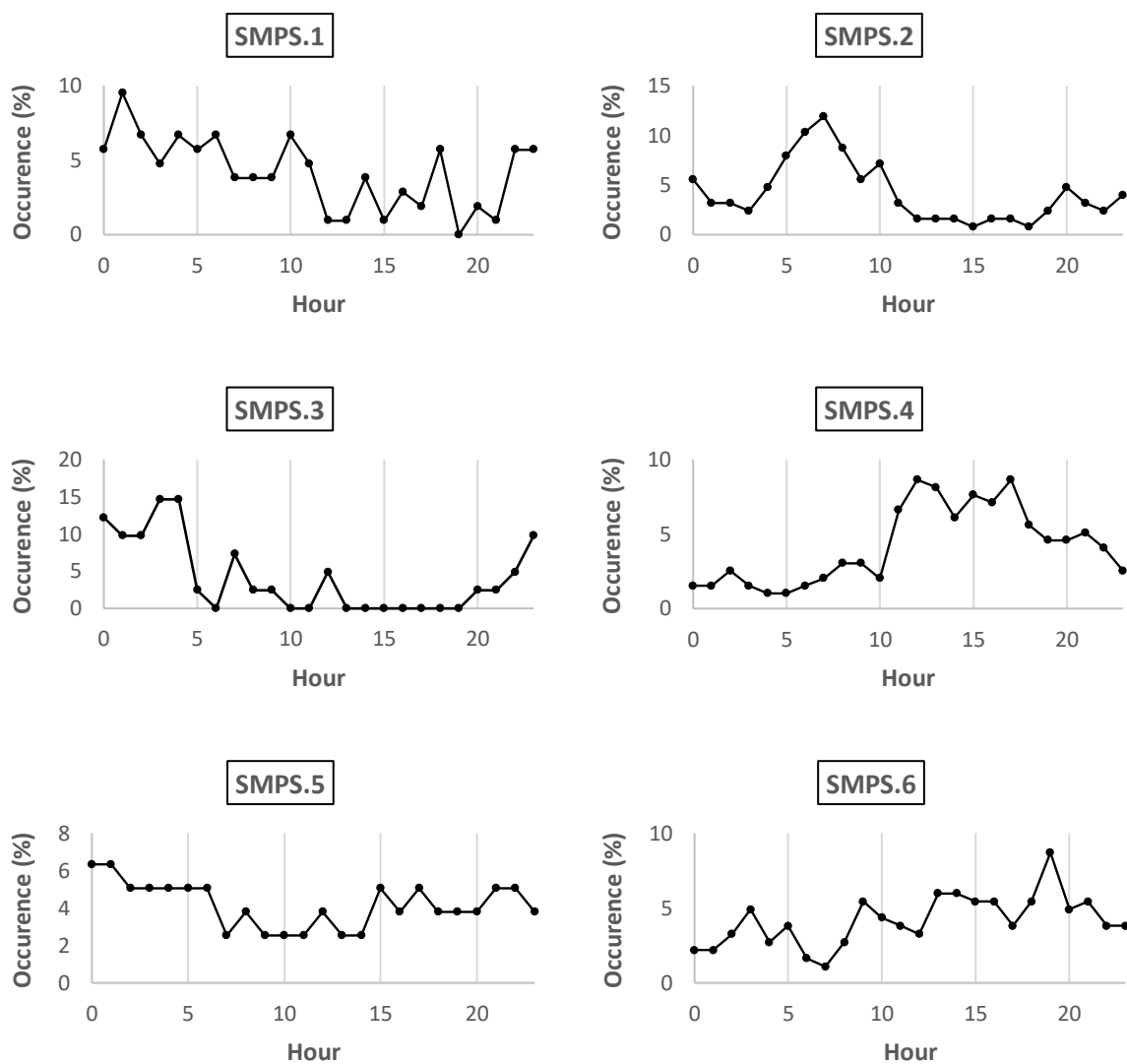
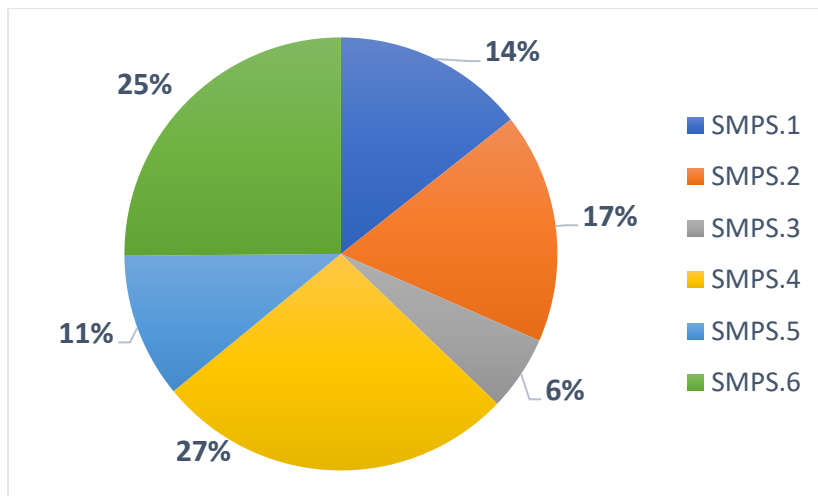


Figure 3: Frequency and diurnal variation of the clusters formed by the SMPS data.

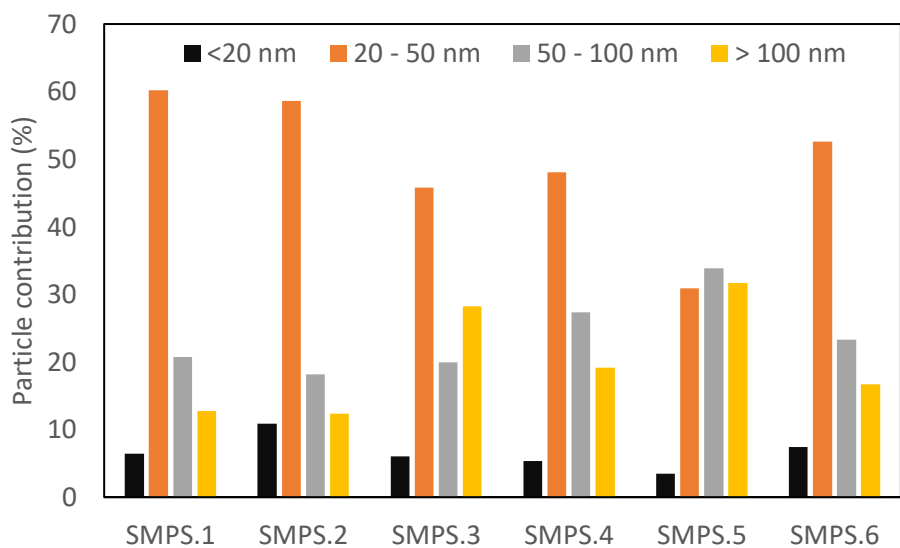
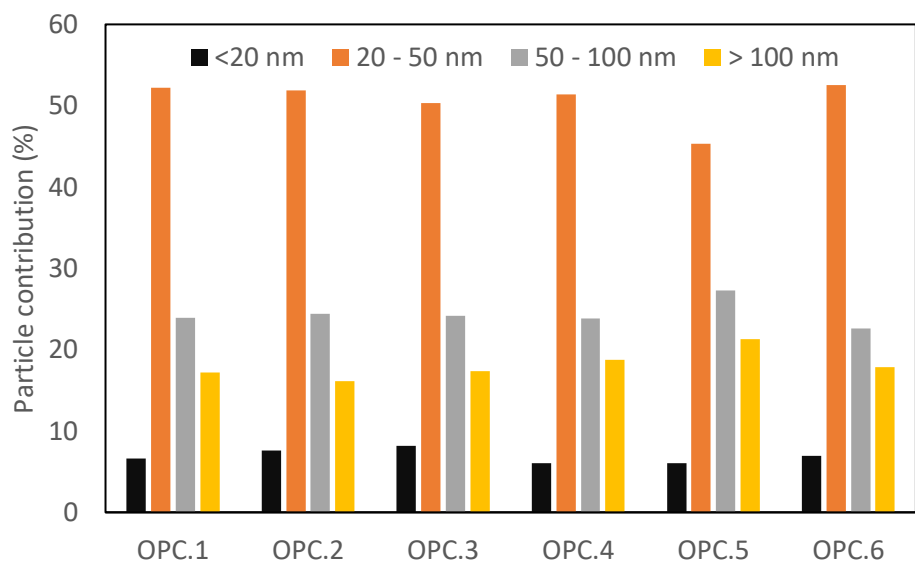


Figure 4: Particle contributions in the range 12 – 550 nm (using the SMPS data), for the clusters formed using the OPC data (top) and the SMPS data (bottom).

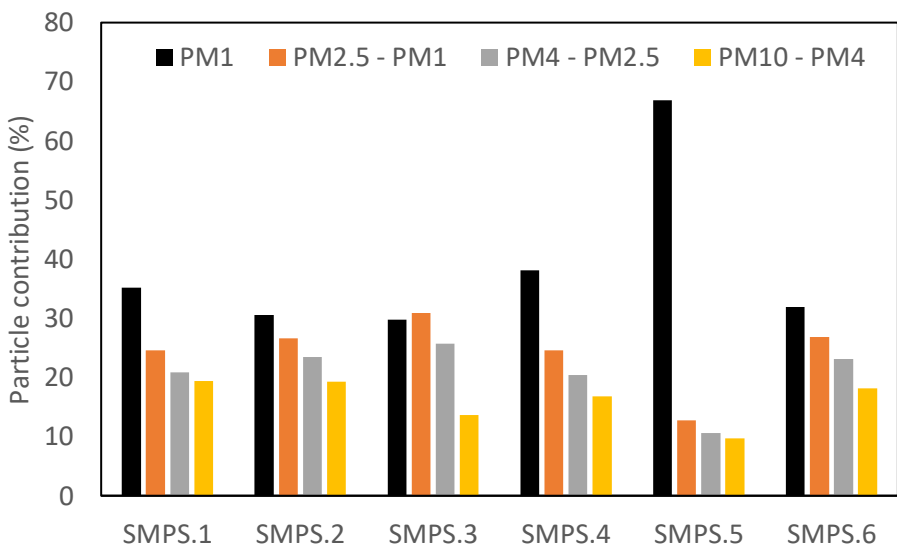
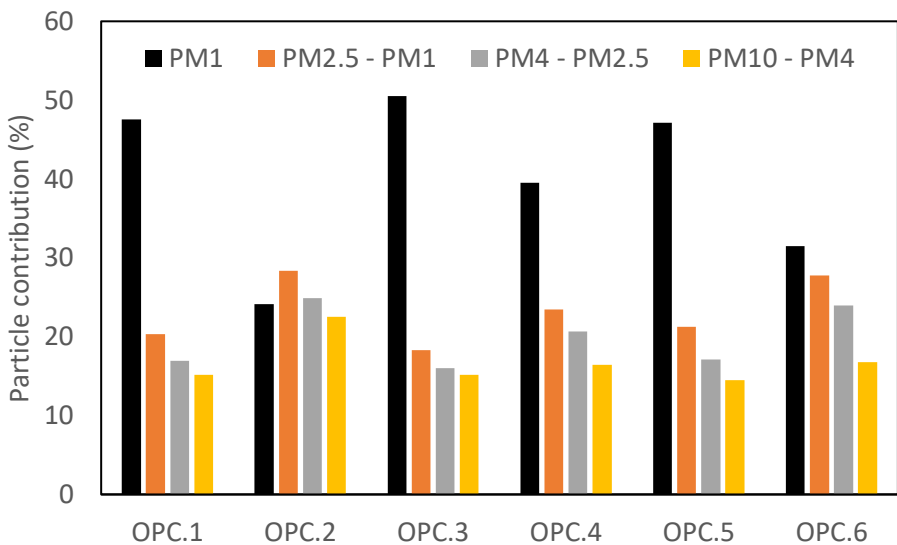


Figure 5: Particle contributions up to $10 \mu\text{m}$ (using the FIDAS data), for the clusters formed using the OPC data (top) and the SMPS data (bottom).

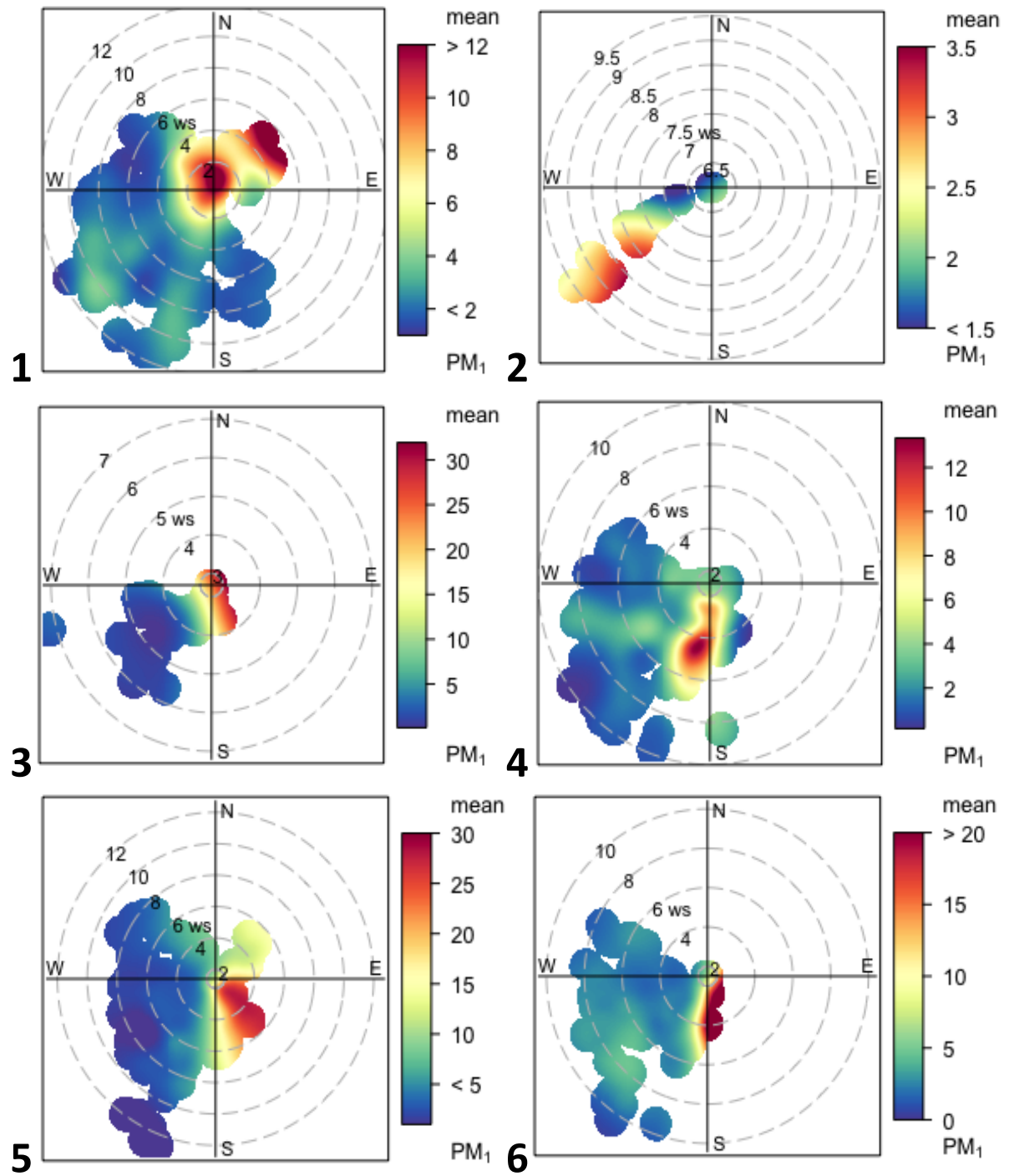


Figure 6: Polar plots for the PM_1 ($\mu\text{g m}^{-3}$) for the clusters formed by the OPC data.

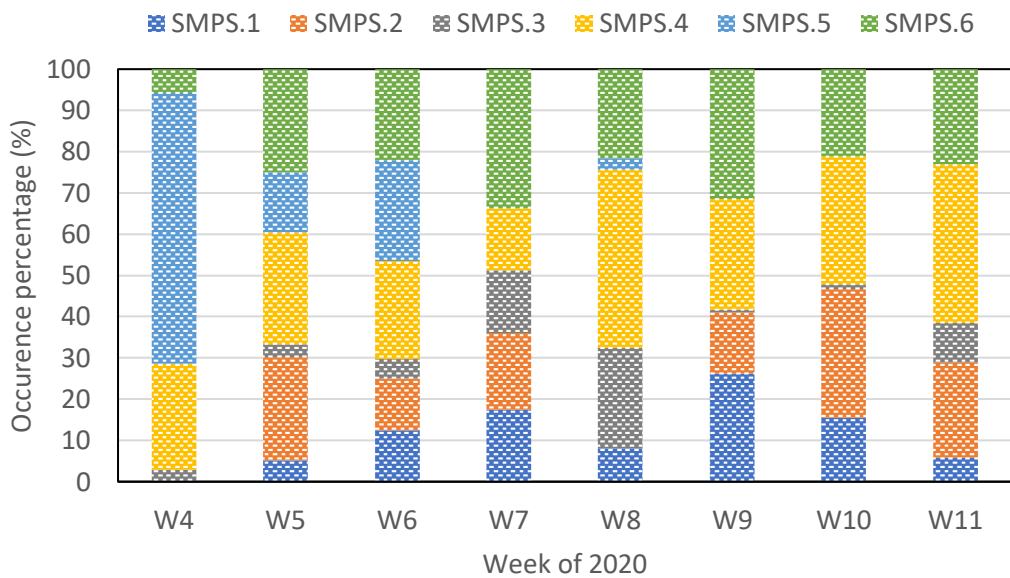
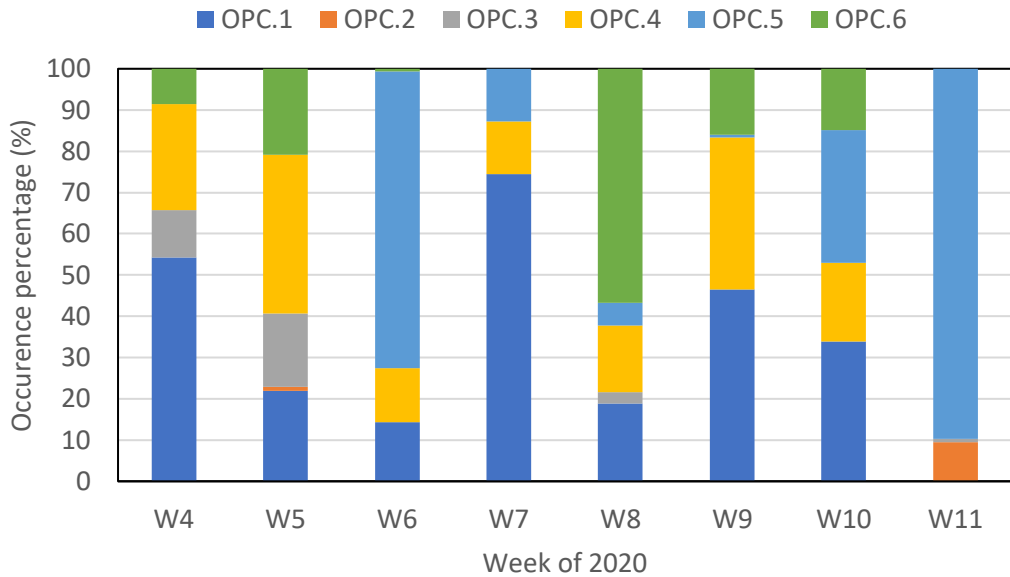


Figure 7: Weekly contribution (week number refers to week of year 2020) of the clusters formed by the OPC (top) and SMPS (bottom).